Proceedings of the
3rd ASME/JSME Joint Fluids Engineering Conference
July 18-23, 1999, San Francisco, California

FEDSM99-7023

NONLINEAR SUBGRID EMBEDDED ELEMENT-FREE GALERKIN METHOD FOR MONOTONE CFD SOLUTIONS

Subrata Roy and Mark Fleming
Technology Center, Case Corporation
7S. 600 County Line Road
Burr Ridge, IL 60521-6975, USA

ABSTRACT

Achieving stable, accurate, monotone and efficient (SAME) discrete approximate solution is of tremendous interest for convection-dominated computational fluid dynamics (CFD) applications. Recently, a non-linear Sub-Grid eMbedded (SGM) finite element basis was developed for generating multidimensional SAME solutions via the weak statement (WS). The theory confirms that only the Navier-Stokes dissipative flux vector term is appropriate for implementing SGM, which thereafter employs element-level static condensation for efficiency and nodal-rank homogeneity. It is based on a genuinely non-linear, non-hierarchical, high-degree finite element basis for use in a discretized approximation of a WS algorithm. In this paper, the SGM methodology is extended to the Element Free Galerkin (EFG) method.

INTRODUCTION

The fundamental challenge in computational fluid dynamics (CFD) algorithm design is creation of discretized methodology possessing accuracy with stability in the presence of solution distributions/discontinuities, as aggravated by the fundamental nonlinearity of the Navier-Stokes partial differential equation (PDE) system. Scientific study emerged some 70 years ago, eventually leading to the Taylor series-based development of the scalar Lax-Wendroff dissipative algorithm. Following, the 1960s witnessed emergence of a wide variety of finite difference CFD algorithms, with stabilization induced by variations thereon, termed *upwind* methods, often leading to first order-accurate algorithms. The associated solutions experienced difficulty in resolving shocks, turbulent flow details, and convection processes with sharp fronts.

Therefore, the elusive CFD algorithm research goal remained to develop a multi-dimensional arbitrary grid algorithm extracting SAME solution on a *practical mesh* for arbitrary Reynolds number. Stabilizing techniques like artificial viscosity methods by Baker and Kim (1987), Lax (1954) and Kreiss and Lorenz (1989) and/or flux correction operations of Boris and Book (1973) and Salezak (1979) contain one or more arbitrary parameters. Flux vector splitting methods of van Leer (1982) replace parameters with switches, but solutions may still exhibit oscillations near strictly local extrema. Techniques utilizing non-linear correction factors called *limiters* require a relatively dense mesh for interpolation to attain an essentially non-oscillatory (ENO) solution (Huynh, 1993). These theories were invariably developed via one-dimensional schemes, and the theory and implementation remains tedious in a multi-dimensional application.

"Adaptive" *p* and *h-p* FE algorithms have been extensively examined by Babuska, et al. (1990), Demkowicz, et al. (1992), Jensen (1992), Johnson and Hansbo (1992), Oden (1994), Zienkiewicz and Craig (1984) and Zienkiewicz et al. (1982). Despite several advantages, including "unstructured meshing," these algorithms add significant cost to operation count and storage requirements that can hinder achieving *practical mesh* solutions. Recent developments in the area of subgrid scale resolution include hierarchical (*h-p*) elements by Zienkiewicz and Zhu (1992) and inclusion of nodeless bubble functions by Hughes (1995). Solution monotonicity is typically not an ingredient in these theories, and as the number of degrees of freedom (DOF) increase, especially for 3-D, the algebraic system matrix order increases rapidly, hence also the computer resource requirement. Numerical linear algebra efficiency then also becomes a central issue.

Meshless methods such as EFG have recently been the topic of a great deal of academic research. The approximation in a meshless method is written in terms of a set of nodes and the boundaries of the model. Since no predefined element connectivities are present, these methods offer hope for problems involving sharp gradients because of their ability to add nodal refinement without subdividing elements. In addition, it is quite easy to enhance the approximation in situations where information is available regarding the form of the solution, such as linear elastic

fracture mechanics (Fleming et. al, 1997). This method has been used extensively for fracture and crack growth in which the meshless nature of the method is very beneficial (Belytschko, Lu, and Gu, 1994). Liu and coworkers have applied meshless methods to problems involving fluid mechanics and shock capturing (Liu and Chen, 1995, Liu et al., 1996).

However, obtaining accurate EFG solutions for problems with sharp gradients typically requires a great deal of nodal refinement, and hence is computationally expensive. As a remedy, we propose a new matrix procedure combining sub-grid embedding (SGM) algorithm and EFG to extract the minimal degree-of-freedom accuracy and monotonicity on arbitrary node distribution that could be useful for both fluid dynamics and structural analysis. The SGM basis construction is distinct from reported developments in the area of subgrid scale resolution, including hierarchical (*h*-*p*) elements and nodeless bubble functions. The SGM development by Roy (1994), Roy and Baker (1997, 1998) employs strictly classical Lagrange basis methodology, and the SGM basis is applicable *only* to the dissipative flux vector term $\mathbf{f}_j^v$ in (1). The discretized kinematic flux vector $\mathbf{f}_j$ remains a "centered" construction via the parent strictly Galerkin weak statement. The key efficiency ingredient of the SGM element is reduction to linear basis element matrix rank for any embedded degree. This is in sharp contrast to conventional enriched basis FE/FD algorithms, as the SGM element strictly contains matrix order escalation, hence increased computer resource demands.

In this paper we document the newly developed theory for the subgrid embedded element-free Galerkin (SGEFG) method that guarantees solution monotonicity via eigenvalue analysis. The EFG approximation is first formulated and then the SGM theory is reviewed and implemented for EFG. The SGEFG method is applied for both linear and non-linear convection-diffusion fluid dynamics problems.

THEOERTICAL DEVELOPMENT

Consider the *d*-dimensional steady state NS conservation law system for state variable $\mathbf{q}=\mathbf{q}(\mathbf{x})$ of the form

$$\frac{\partial}{\partial \mathbf{x}}\left(\mathbf{f}_u^x + \mathbf{f}_u^x\right) - s = 0, \text{ on } \Omega \times t \subset R^d \times R^+, \mathbf{x} \equiv x_j, \ 1 \le j \le d \quad (1)$$

where $\mathbf{f} = f(\mathbf{u}, \mathbf{q})$ and $\mathbf{f}^v = f\left(e \frac{\partial \mathbf{q}}{\partial \mathbf{x}}\right)$ are kinetic and dissipative flux vectors respectively, the convection velocity is $\mathbf{u}$, $e > 0$ is the diffusion coefficient that varies parametrically and s is a source. Appropriate initial and boundary conditions close system (1) for the well-posed statement.

The analytical solution to (1) is smooth, monotone and bounded. However, computational difficulties occur as ε leading to occurrence of "thin layer" solutions containing large gradients, *e.g.*, wall layer, shock. This is the natural occurrence in CFD for a large Reynolds number (Re). Here an oscillatory error mode dominates the spatially discretized CFD solution process leading to instability in the presence of the inherent Navier-Stokes non-linearity in **f**.

Element Free Galerkin (EFG) Method

The approximation of the general field variable **q(x)** at any point **x** in the domain Ω is written

$$\mathbf{q}(\mathbf{x}) = \mathbf{p}^T(\mathbf{x})\mathbf{a}(\mathbf{x}) \quad (2)$$

where **p(x)** is a basis and **a(x)** is a vector of unknown coefficients. In one dimension, we have used

$$\begin{aligned} \mathbf{p}^T(x) &= \begin{bmatrix} 1 & x \end{bmatrix} \quad \text{linear basis} \\ \mathbf{p}^T(x) &= \begin{bmatrix} 1 & x & x^2 \end{bmatrix} \quad \text{quadratic basis} \end{aligned} \quad (3)$$

To write the approximation of the field variable $q(x)$ in terms of nodal coefficients, a moving least squares methodology is employed (see Lancaster and Salkauskas, 1981). An L_2 norm can be written as

$$J = \sum w(x - x_{\mathbf{I}})\left[\mathbf{p}^T(x_I)\mathbf{a}(x) - q_I\right]^2 \quad (4)$$

where q_I is a set of nodal coefficients and $w(x-x_I)$ is a weight function centered at node *I*. We have used a Gaussian weight function

$$w(d_I) = \begin{cases} \dfrac{\exp\left(-(d_I/c)^2\right) - \exp\left(-(d_{mI}/c)^2\right)}{1 - \exp\left(-(d_{mI}/c)^2\right)} & d_I \le d_{mI} \\ 0 & d_I > d_{mI} \end{cases} \quad (5a)$$

$$d_{mI} = d_{max} * c_I, \quad \text{and} \quad c = a * c_I \quad (5b)$$

where $d_I = ||x - x_I||$ is the distance from node x_I to a sampling point x and d_{mI} is the domain of influence for node *I* and the parameter c is the dilation parameter (Fleming, et al., 1996). The characteristic nodal spacing, c_I, is used to define these parameters and d_{max} and a are constants. We have set c_I equal to the distance to the second nearest neighboring node. For the Gaussian weight function in (5a), it is recommended that $d_{max}/a \ge 4$.

The minimum of J with respect to $\mathbf{a}(x)$ leads to

$$q(x) = \sum_{I=1}^{n} \mathbf{p}^T(x)\mathbf{A}^{-1}(x)\mathbf{C}_I(x)\,q_I = \sum_{I=1}^{n} N_I(x) q_I$$

where $N_I(x)$ is the shape function and

$$\begin{aligned} \mathbf{A}(x) &= \sum_{I=1}^{n} w(x - x_I)\mathbf{p}^T(x_I)\mathbf{p}(x_I) \\ \mathbf{C}(x) &= \left[w(x-x_1)\mathbf{p}(x), w(x-x_2)\mathbf{p}(x), \ldots . w(x-x_n)\mathbf{p}(x_n)\right] \\ \mathbf{q} &= \left[q_1, q_2, \ldots\ldots\ldots, q_n\right] \end{aligned} \quad (6)$$

(see Belytschko, Lu and Gu, 1994, and Belytschko and Fleming, 1999).

Sub-Grid Embedding (SGM) Theory

Independent of the generality of the flux vectors and dimension *d*, the *weak form* of (1) always produces a nodal-order ordinary differential equation (ODE) system consisting of a mass matrix [*M*] from the time derivative, a velocity matrix [*U*] from the convective flux vector and a diffusion matrix [*D*] from the dissipative flux vector. In standard methods, for a basis function $\{N_k\}$ of Lagrange polynomial order *k*, the element level diffusion matrix $[D_k]_e$ is defined as

$$\left[D_k\right]_e = \int_{\Omega_e} \frac{\partial\{N_k\}}{\partial \mathbf{x}} \frac{\partial\{N_k\}^T}{\partial \mathbf{x}} dt, \quad 1 \le j \le d \qquad (7)$$

The SGM theory augments the diffusion term in WS via an *embedding* function $g_S(\mathbf{x},\mathbf{c})$, hence the name "SubGrid eMbedded." The embedded polynomial contains one definable parameter $\mathbf{c}$ for each additional Lagrange degree $k>1$. A key ingredient of this embedding process involves static condensation as described in Roy and Baker (1997). The final form of the SGM element-like basis set $\{N_S\}$ for $k=2=S$ is expressed in 1-D, analogous to the $k=1$ Lagrange basis, as

$$\{N_S\} = \begin{Bmatrix} 1-m \\ m \end{Bmatrix}, \text{ but } m = \sum_{i=1}^{\infty} a_i V_i^a \qquad (8)$$

In (8), m is a polynomial function of an expansion coefficient set, a_i, dependent on embedding degree k, and the $k=1$ element local coordinate $z(x)$ and $\alpha=f(c)$. The discussion in Roy and Baker (1997) confirms $c\ge1$ is the requirement. For general applications, a nodally distributed SGM parameter $r_I(c)$ on node I is defined in Roy and Baker (1997). For the node where $r_I<1$, the value is averaged from the neighboring nodes. The Lagrange linear ($k=1$) and quadratic ($k=2$) FE basis polynomial set, the $k=1$, $p=2$ hierarchical (bubble) element, and the SGM $S=2$ ($k=2$, reduced) Lagrange element for 1-D and 2-D are compared in Figure 1a-f.

The form of r_I, a theoretically *non-linear* monotonicity constraint, is determined via (1) leads to a theoretically *non-linear* monotonicity constraint via enforcement of a real eigenvalue spectrum for the algorithm stencil of a 1-D model SGM element form. Thereby, the theory predicts the optimal distribution of the SGM embedded parameter (set) on each element, hence the mesh Ω^h. The generalization to non-uniform, d-dimensional discretizations leads to the potential for attainment of nodally exact monotone solutions on arbitrary meshes. The multidimensional form of the nodally distributed SGM solution monotonicity constraint r_I (RSGM) is directional and the parameter is derived as a function of convection velocity, mesh projection and Re. Verification for both linear and non-linear convection-diffusion equation SGM solutions is documented in Roy and Baker (1997), c.f. Figure 2, where for a small e ($O10^{-5}$) SAME nodally accurate solutions are obtained on very coarse meshes.

For general applications in 1-D, a nodally distributed (subscript I) SGM parameter is preferable to an element parameter. Therefore, defining $r_I = (2c_I+1)/3$ the monotonicity constraint form becomes

$$\frac{2c_I+1}{3} \equiv r_I \ge \frac{h_I|u_I|}{eF} = \frac{h_I|u_I|\,\mathrm{Re}}{F} \qquad (9)$$

where Reynolds number Re replaces e and $F>0$ is a real number. In 1-D, F is precisely determined from the eigenvalue analysis, hence $F=2$ for the linear convection-diffusion (Peclet) problem, $F=6$ for the linear stationary wave definition, while $F=3$ for non-linear convection-diffusion (viscous Burgers) equation (Roy, 1994). However, for $d>1$ multidimensional problems, determining a suitable functional form for F involves definition of a correlation function $F_{Ij}= f(\mathrm{Re}, \det_e)$, the form of which must be validated.

For velocity field $\mathbf{u}_I = (u_{I1}, u_{I2}, u_{I3})$, principal coordinate mesh measures h_{I1}, h_{I2} and h_{I3} and principal coordinate diffusion parameter set $\boldsymbol{\varepsilon} \Rightarrow (e_{I1}, e_{I2}, e_{I3})$, the condition for a d-dimensional monotone solution is expressed for scalar components of $\mathbf{r}_I = (r_{I1}, r_{I2}, r_{I3})$, in (9) and this correlation function F_{Ij} is

$$r_{Ij} \ge \frac{|u_{Ij}|h_{Ij}}{F_{Ij}e_{Ij}}, \; F_{Ij} = \left(\frac{AV_e}{e_{Ij}^{d-1}h_{Ij}}\right)^{1/d}, 1 \le j \le d, \; 1 \le I \le \text{No. of nodes} \qquad (10)$$

Hence, only the scalar $0<A<2$ remains undefined, and must be estimated. V_e ($=2^d\det_e$) is the volume (area) of the d-dimensional element, and the form for F_{Ij} was determined using computational data from the 2-D and 3-D linear Peclet problem solutions (Roy and Baker, 1998).

Sub-Grid eMbedded Element Free Galerkin (SGEFG) solution process :

The steps forming the SGM augmented EFG WS^h solution process include:

1. Formulate the EFG algorithm as in (2)-(8).
2. Use the monotonicity constraint (9)-(10) to compute $\mathbf{c}_I$ or $\mathbf{r}_I$ or estimate $r_{Ij} = f(u_{Ij}, h_{Ij}, \mathrm{Re})\ge1$. For the node where r_I, r_{Ij} <1, the value is averaged from the neighboring nodes.
3. Form the SGM augmented element-like diffusion matrix $\left[D\right]_e = \int_{\Omega_e} g_2(\mathbf{r}) \frac{\partial\{N_S\}}{\partial \mathbf{x}} \frac{\partial\{N_S\}^T}{\partial \mathbf{x}} dt$, where $g_2(\mathbf{r})=\{G\}^T\{N_2\}$, and $\{G\}^T=\{1,c_x,1\}\otimes\{1,c_y,1\}\otimes\{1,c_z,1\}$.
4. Rank reduce $[D]_e$ to $[D_S]_e$ via static condensation as described in Roy and Baker (1997).
5. Form the weak statement WS^h for the discretized domain Ω^h.
6. Solve for the numerical linear algebra.
7. Return to step 1 and repeat process until solution converges to a negligible residual.

RESULTS AND DISCUSSION

Computational experiments are presented to demonstrate the advantages of SGEFG algorithm for problems involving sharp gradients. Documentary computational results verify theory and summarize performance for a range of linear and nonlinear verification and benchmark problems that model the character of solutions to the Navier-Stokes equation system. For the EFG method, the parameters d_{max} = 2.01 and a = 0.5 in (5b) are used for these examples.

***Linear Stationary Wave* ($u \to 0$, $e \to 0$, $s=0$)**

The governing parabolic differential equation is

$$\frac{d}{dx}\left(uq - e\frac{dq}{dx}\right) = 0, \quad \text{on } -\ell \le x \le \ell \qquad (11)$$

The analytical solution to (11) as parameterized by the familiar "Reynolds number", Re=ul/e, is of the form $q(x)$=A+B exp(xuRe). For the Dirichlet boundary conditions $q(0)$=-1 and $q(1)$=1, the analytical solution is

$$q(x) = \frac{1 + e^{u\mathrm{Re}} - 2e^{xu\mathrm{Re}}}{1 - e^{u\mathrm{Re}}} \qquad (12)$$

As Re becomes large, $q(x)$ approaches a step function equal to unity ahead of the front u=-1 and q=-1 behind the u=1 front. The slope of the solution q at the front is

$$\frac{dq}{dx} = -\frac{2u\,\mathrm{Re}\, e^{xu\mathrm{Re}}}{1 - e^{u\mathrm{Re}}}; \quad \text{as } \mathrm{Re} \to \infty, \ \frac{dq}{dx} \to \mathrm{Re} \qquad (13)$$

Clearly, for large Re, as $|u| \to 0$, at the wave intersection, $|q|$ approaches 0 and the solution becomes highly singular near the region where u changes sign.

As Reynolds number increases, achieving a monotone, accurate approximate solution becomes increasingly difficult. For standard finite element (or finite difference) methods, this has been traditionally handled by including artificial diffusion. For this verification case, the standard FEM solution with k=1, p=0 for Re=10^6 is totally dispersive on meshes up to 1001 nodes (see Roy and Baker, 1997). Even the EFG solution in Figure 3a shows error oscillation dominant in the domain.

In distinction, for the comparison SGEFG g_2 optimal choice r, Re=10^6, on the uniform 21 node mesh, yields an absolute monotone nodally-exact solution, Figure 3b. For this problem definition, F=6 in (9) and the theoretical prediction of the subgrid embedding parameter corresponding to Re=10^6 and h=1/20 is r=25000/3 or c=24999/2. Table 1 documents the comparison element and system matrices for standard EFG and SGEFG g_2 choice. Via (13), the analytical end fluxes for (11) are exactly zero for any large Re. While the standard EFG solution predictions for these fluxes are highly erroneous (almost three orders of magnitude error), the SGEFG g_2 choice yields end fluxes accurate to machine precision.

***Non-linear stationary wave* ($u \neq 0$, $e \to 0$, s=0)**

The non-linear form of (11) results from the definition of $q \equiv u$, hence

$$u\frac{du}{dx} - \frac{d}{dx}\left(e\frac{du}{dx}\right) = 0, \quad \text{on } -\ell \le x \le \ell \qquad (14)$$

The nondimensional form of the above 1-D stationary viscous Burgers equation (14) introduces the Reynolds number in the viscous term and for u=1 at x=-1 and u=-1 at x=1, the analytical solution to (14) is

$$u(x) = \tanh\left(-\frac{x\,\mathrm{Re}}{2}\right) \qquad (15)$$

and corresponding slope is

$$\frac{du}{dx} = -\frac{2u\,\mathrm{Re}\, e^{xu\mathrm{Re}}}{1 - e^{u\mathrm{Re}}}; \quad \text{as } \mathrm{Re} \to \infty, \ \frac{dq}{dx} \to +\mathrm{Re} \qquad (16)$$

A detailed discussion of standard FEM solution procedures for the unsteady Burgers equation may be found in Baker (1983, Ch. 4.14) and Roy and Baker (1997).

As Re becomes large, the iterative algebraic solution process for (14) becomes highly unstable, as the dispersive error mode totally corrupts the entire solution process. Figure 4 summarizes computed solution character for this problem for Re=10^3. The initial condition is a symmetric ramp as shown in Figure 2. Figure 4a illustrates the nonlinear instability present for the standard EFG solutions, stopping iterative convergence at δ<0.001. Although the quadratic basis degree standard FEM solution has reduced oscillations by about 25% in Roy and Baker (1997), the solution remains unsatisfactory even for a 2000 node uniform mesh. The corresponding EFG solution in Figure 4a is also very oscillatory even on a 101 node mesh. In distinction, for the nodally adaptive SGEFG g_2 choice and for F=3, an *optimal* 21-node uniform mesh yields a monotone, nodally exact solution for Re=10^5, Figure 4b. The corresponding SGEFG solution iteration process is stable and convergent to δ<0.000001.

***Linear advection-diffusion with source* ($u \neq 0$, $e \to 0$, $s \neq 0$)**

The problem definition is similar to (11) except for the source terms, s, on the right hand side.

$$u\frac{dq}{dx} - \frac{d}{dx}\left(e\frac{dq}{dx}\right) = s, \quad \text{on } -\ell \le x \le \ell \qquad (17)$$

The analytical solution for the nonhomogeneous equation (17) is clearly a function of the source term s. For our consideration, the source s can be any spatial function, e.g. s=Ax^2+Bx+C, where A=10$e^{x-0.5}$, B=20sin(x-0.5), and C=10cos(x-0.5sin(x)). The particular solution to (17) for this source function is

where coefficients AL=A/(3uRe); BL=B/(2uRe)+A/(uRe)^2;

$$q = -\frac{2 + \mathrm{AL} + \mathrm{BL} - \mathrm{CL}}{1 - e^{u\mathrm{Re}}} e^{xu\mathrm{Re}} + \frac{1 + \mathrm{AL} + \mathrm{BL} - \mathrm{CL} + e^{u\mathrm{Re}}}{1 - e^{u\mathrm{Re}}} \qquad (18)$$
$$- \mathrm{AL}x^3 - \mathrm{BL}x^2 + \mathrm{CL}x$$

and CL=2A/(uRe)^3+B/(uRe)^2-C/(uRe). For this test case, we used Re=10^3 and the dirichlet boundary $q(0)$=-1 and $q(1)$=1. The EFG algorithm computational solution to this problem as documented in Figure 5 shows the dispersive error wave is present on 101 node mesh while the corresponding SGEFG solution shows an oscillation free solution on a coarse 21 node mesh.

CONCLUSIONS

The presented results confirm the theory for incompressible Navier-Stokes applications. In comparison to other theories for generating higher-order accurate and/or monotone solutions, the SGEFG algorithm advantages include guaranteed (non-linear) monotone solution, excellent conditioning of the *minimum-band* system matrix, and *improved stability* via retained diagonal dominance. Further,

the SGEFG methodology permits retention of lexicographic ordering for any embedding degree, hence exhibits the efficiency of strictly linear basis (or centered FD) algorithms. The SGEFG algorithm thus exhibits the potential for fundamental impact on CFD as well as structural problems, via its intrinsic non-linearity and guarantee of minimum computer memory and CPU requirements for high accuracy monotone solutions on relatively coarse 3-D meshes. Extension of the SGEFG to higher dimensional problem specification is an obvious next step.

Table 1. Comparison for linear advection-diffusion results of EFG and SGEFG for Re=10^6 on 21 node mesh.

21 node mesh	EFG	SGEFG
System matrix near the central node	[0.0 0.5 0.0] [-0.5 1.0 -0.5] [0.0 0.5 0.0]	[1.0 0.0 0.0] [-1.0 1.0 0.0] [0.0 -1.0 1.0]
Solution vector $\{q\}^T$	[… .009 108.3 0.0 -108.3 -.009 …]	[…-1 -1 0 1 1…]
Boundary fluxes [left, right]	[7 -7]	[0 0]

REFERENCES

Babuska, I., B.Q. Guo and E.P. Stephan, 1990, Math. Meth. Appl. Sci., Vol. 12, pp. 413-427.

Baker, A.J. and J.W. Kim, 1987, Int. J. for Num. Methods in Fluids, Vol. 7, pp. 489-520.

Boris, J.P. and D.L. Book, 1973, J. Comput. Phys., Vol. 11, pp. 38-69.

Belytschko, T., Y.Y. Lu, and L. Gu, 1994, Element-free Galerkin Methods, Intl J Num Meth Engg., 37, pp. 229-256.

Belytschko, T. and M. Fleming, 1999, Smoothing, enrichment and contact in the element-free Galerkin method, Comp and Structures, (in press).

Demkowicz, L., A. Karafiat and J.T. Oden, 1992, Comput. Meth. Appl. Mech. Eng, Vol. 101, pp. 251-282.

Fleming, M., Y.A. Chu, B. Moran and T. Belytschko, Int. J. Num. Methods in Engrg., vol. 40, pp. 1483-1504, 1997.

Hughes, T.J.R., 1995, Comput. Meth. Appl. Mech. Eng, Vol. 127, pp. 387-401.

Huynh, H.T., 1993, SIAM J. Numer. Anal., Vol. 30, pp. 57-100.

Jensen, S., 1992, Comput. Meth. Appl. Mech. Eng., Vol. 101, pp. 27-41.

Johnson, C. and P. Hansbo, 1992, Comput. Meth. Appl. Mech. Eng., Vol. 101, pp. 143-181.

Kreiss, H.O. and J. Lorenz, 1989, Initial-Boundary Value Problems and the Navier-Stokes equations, Academic Press, New York.

Lancaster, P. and K. Salkauskas, 1981, Surfaces generated by moving least-squares methods, Math. Comput., Vol. 37, pp. 141-158.

Lax, P.D., 1954, Comm. Pure Appl. Math., Vol. 7, pp. 159-193.

Liou, M.S. and B. van Leer, 1988, Tech. AIAA 88-0624, 26th Aerospace Meeting.

Liu, W.K. and Y. Chen, 1995, Wavelet and multiple scale reproducing kernel methods, Intl J Num Meth Fluids, 21, pp. 901-931.

Liu, W.K., Y. Chen, C.T. Chang, and T. Belytschko, 1996, Advances in multiple scale kernel particle methods, Comp. Mech.

Oden, J.T., 1994, Comput. Meth. Appl. Mech. Eng., Vol. 112, pp. 309-331.

Roy, S., 1994, On Improved Methods for Monotone CFD Solution Accuracy, PhD Thesis, The University of Tennessee.

Roy, S. and A.J. Baker, 1997, Int. J. Numer. Heat Transfer, Vol. 31, pp. 135-176.

Roy, S. and A.J. Baker, 1998, Int. J. Numer. Heat Transfer, Vol. 33, pp. 5-36.

Salezak, S.T., 1979, J. Comput. Phys., Vol. 31, pp. 355-362.

van Leer, B., 1982, Proc. 8th Int. Conf. on Numerical Methods in Fluid Dynamics, Springer-Verlag.

Zienkiewicz, O.C., D.W. Kelly, J. Gago and I. Babuska, 1982, The Mathematics of Finite Elements and Applications IV, J. Whiteman (ed.), pp. 311-346.

Zienkiewicz, O.C. and J.Z. Zhu, 1992, Comput. Meth. Appl. Mech. Eng., Vol. 101, pp. 207-224.

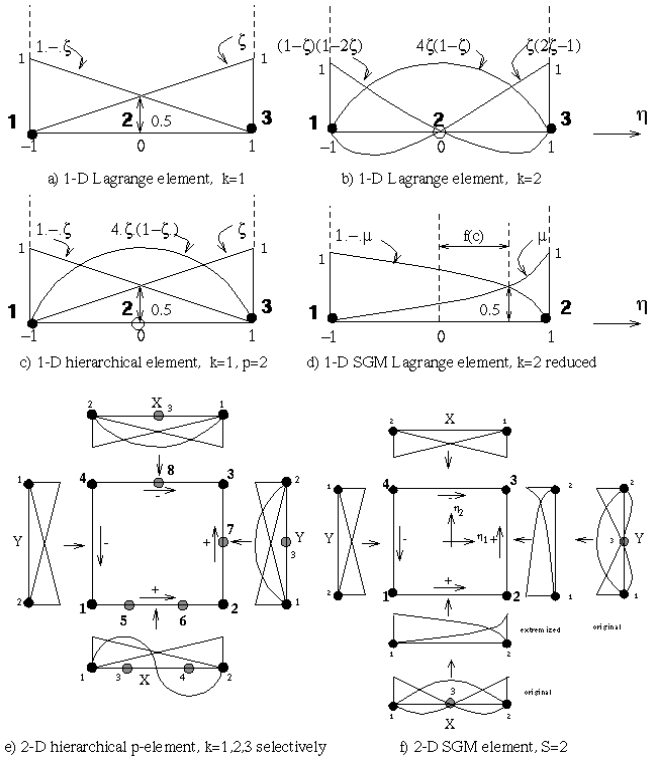

Figure 1: Comparison between standard, hierarchical and SGM elements.

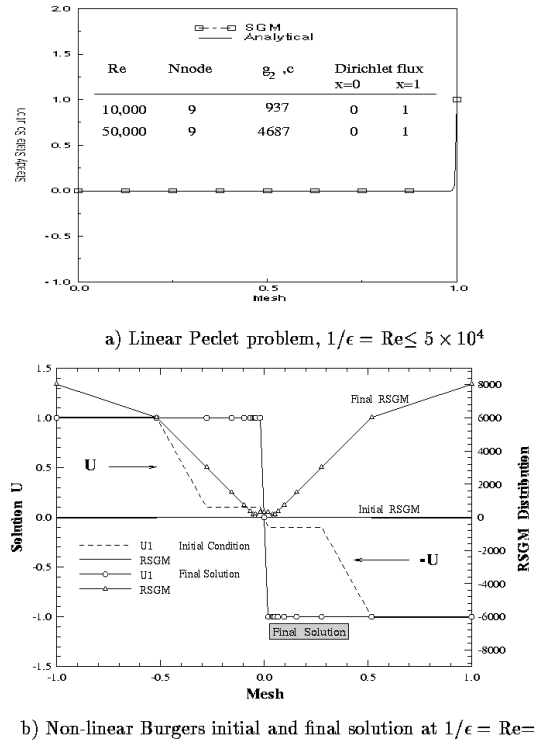

Figure 2: Steady state SGM element SAME solution for 1-D linear and non-linear convection-diffusion problems.

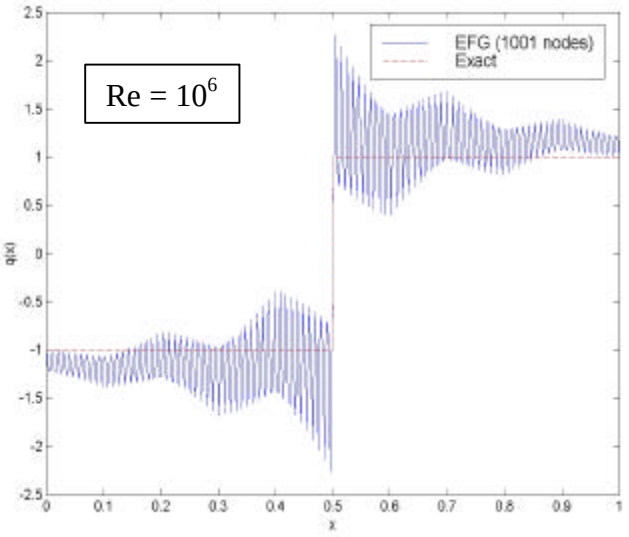

a) Solution with 1001 nodes.

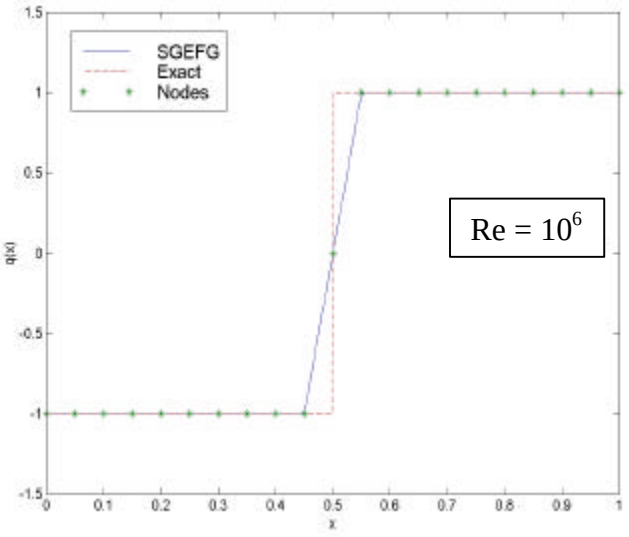

b) Solution with 21 nodes.

Figure 3: Results for a linear stationary wave with EFG and SGEFG methods. For the solution with 21 nodes, the EFG solution was extremely oscillatory and is not shown.

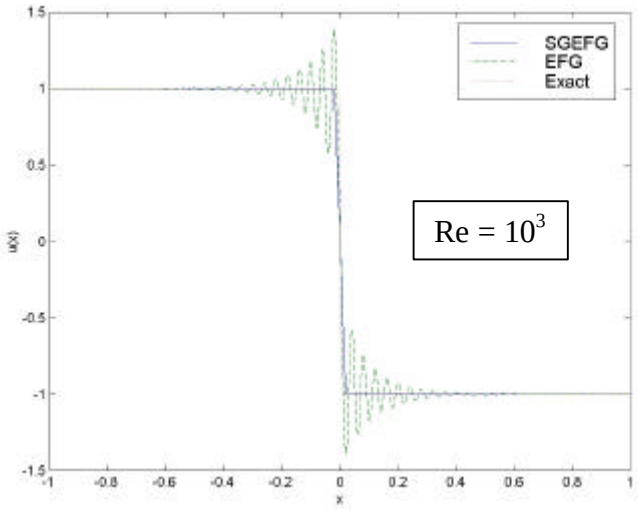

a) Solution with 101 nodes.

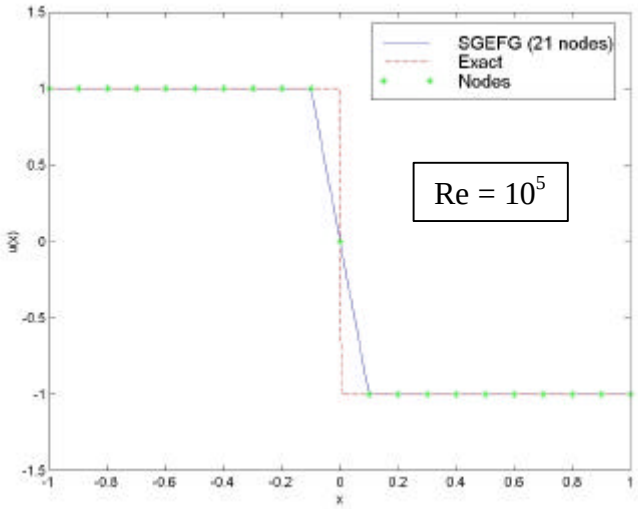

b) Solution with 21 nodes.

Figure 4: Solution for a non-linear stationary wave (Burgers equation) by EFG and SGEFG methods. The solution is not plotted for EFG with Re = 10^5 due to the severe oscillations.

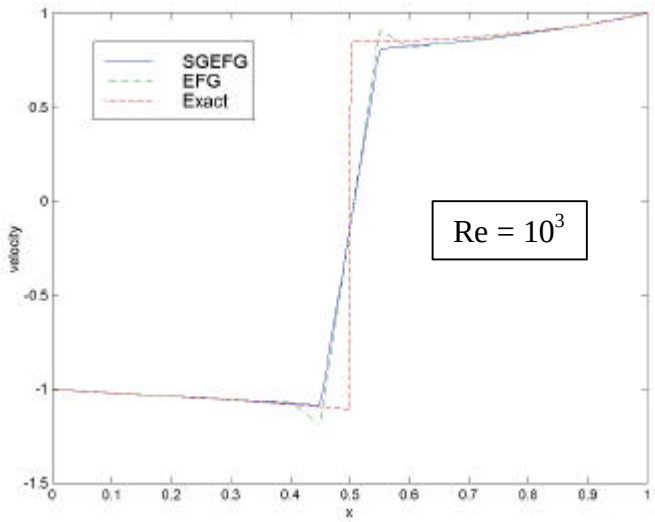

Figure 5: Solution to the linear advection-diffusion equation with a source term.